On reliability of finite element method in fluid-structure interaction problems *

Petr Sváček
Faculty of Mechanical Engeneering, Czech Technical University in Prague, Department of Technical Mathematics, Karlovo nám. 13, 121 35 Praha 2

Abstract. In this paper we are concerned with numerical methods for fluid-structure interaction (FSI) problems and with their verification and validation. The fluid-structure interaction modelling is very complicated problem, where the most complicated and cruicial part is modelling of the fluid flow. Therefore the main interest of this paper is the numerical approximation of two dimensional incompressible viscous fluid over a flexibly supported profile. In technical problems the relevant Reynolds numbers are usually very high ($10^4 - 10^6$) and the fluid flow is turbulent. The correct numerical approximation requires very fine mesh refining as well as very small time steps involved in the computation. On the other hand in many technical applications the Reynolds Averaged Navier-Stokes equations are being used together with a suitable turbulence model. Here, both (laminar) Navier-Stokes equations as well as Reynolds Averaged Navier-Stokes equations are considered, numerically approximated by the Finite Element Method (FEM), stabilized by Galerkin-Least-Squares technique, and the obtained solution compared to the experimental data.

Keywords: aeroelasticity, Reynolds Averaged Navier-Stokes equations, Navier-Stokes equations

Nomenclature

$L(t), D(t), M(t)$	=	aerodynamic lift and drag force and torsional moment
m	=	mass of the airfoil
S_α, I_α	=	static and inertia moments around the elastic axis EO
$k_{hh}, k_{\alpha\alpha}$	=	bending and torsional stiffness
l, c	=	airfoil depth and chord
α, h	=	rotational and vertical displacements around the elastic axis EO
$\mathcal{G}_t$	=	computational domain occupied by fluid at time t
$\partial\mathcal{G}_t$	=	boundary of the domain $\mathcal{G}_t$
P	=	time averaged kinematic pressure,
ρ, ν	=	constant fluid density and (laminar) kinematic viscosity of the fluid
ν_T	=	turbulent kinematic viscosity
τ_{ij}, σ_{ij}	=	fluid stress tensor and Reynolds stress tensor
Ω_{ij}	=	tensor rotation of the fluid velocity

* This research was supported under grant No. 201/05/P142 of the Czech Grant Agency and under Research Plan MSM 6840770003 of the Ministry of Education of the Czech Republic.

1. Introduction

The fluid-structure interaction problems can be met in many technical applications (for details see, e.g., (Dowell, 1995; Naudasher and Rockwell, 1994)). The treatment of fully coupled interaction problem of a structure and fluid flow is very difficult. Therefor, it is usually modelled with several simplifications. The main objective of commercial codes (as, e.g., NASTRAN) is to determine the critical fluid flow velocity. The post-flutter behaviour can not be captured. The special problems of aero-elasticity mainly in linear domain are solved.

The paper focus on numerical simulations of two dimensional viscous incompressible air flow around an airfoil. The main objective is the correct numerical resolution of the flow and the fluid forces acting on the airfoil. The relevant flow velocities for the selected class of problems are in the range $0-120$ m s^{-1}. The flow is described by the incompressible Navier-Stokes equations. The other possibility is to use the model of compressible flow. Nevertheless, the numerical approximation of low Mach number flows at incompressible limit is quite complicated and a modification of governing equations has to be used.

The numerical approximation of incompressible flow can be carried out with the use of various methods. In CFD, the finite volume method is rather popular. In our paper the finite element method is used for the spatial discretization of the problem. In this case several sources of instabilities have to be treated. First, in order to guarantee the stability of the scheme the finite elements for velocity and pressure need to be selected in a proper way to satisfy the Babuka-Brezzi condition. Moreover, very high Reynolds numbers result in the appearance of spurious oscillations in the approximate solution. In last decades a number of stabilization procedures have been developed. In this paper the stabilization based on GLS (Galerkin Least-Squares) method together with grad-div stabilization is employed. The combination of this method with the mesh refinement (e.g., performed by the anisotropic mesh generator, see (Dolejší, 2001)) results in a very robust and efficient method. The choice of stabilization parameters is based on the numerical analysis of the problem as well as numerical experience, see (Lube, 1994), (Sváček and Feistauer, 2004). The presented method is applied to the solution of incompressible (laminar) Navier-Stokes equations and also to the solution of Reynolds Averaged Navier-Stokes (RANS) equations. In this paper the application of the finite element method to RANS system of equations is discussed. For the description of application onto (laminar) Navier-Stokes equations, see (Sváček, Feistauer, and Horáček, 2004). The Reynolds stresses involved in the RANS equations are modelled with the aid of the Spallart-Almaras turbulence model (for an overview of turbulence models used in computational fluid dynamics, see, e.g. (Wilcox, 1993).

The structure motion is simulated by the solution of a system of nonlinear ordinary differential equations for the vertical and angular displacements. The airfoil motion results in deformations of the computational domain, which are treated with the aid of Arbitrary Lagrangian-Eulerian(ALE) method, see (Nomura and Hughes, 1992), (LeTallec and Mouro, 1998).

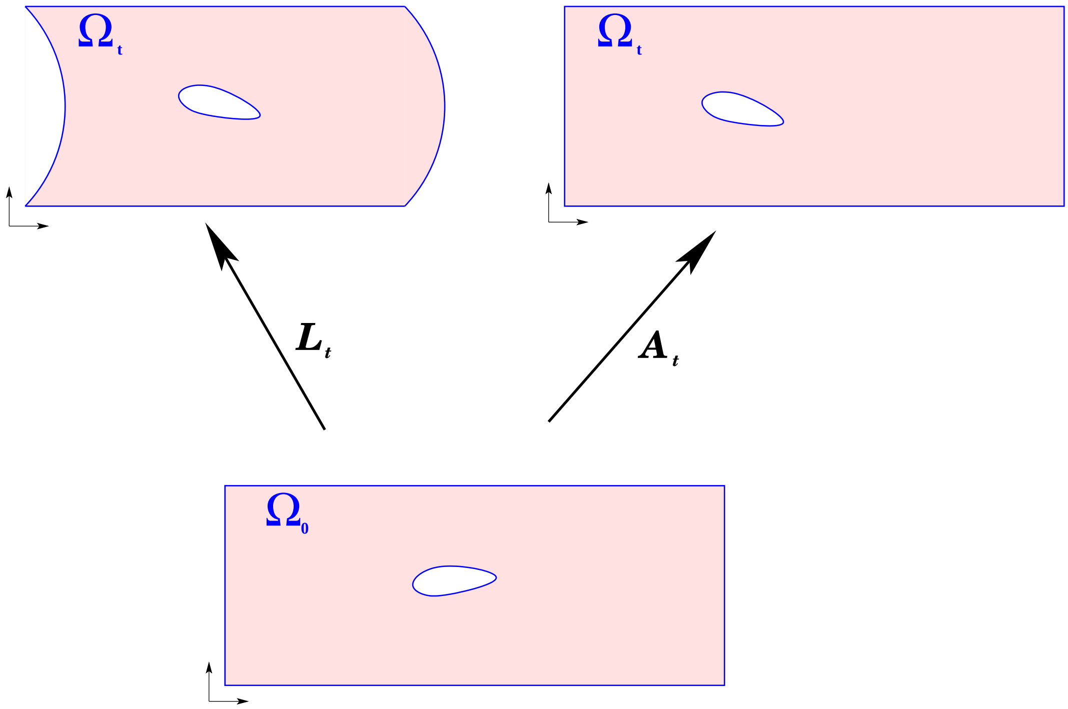

Figure 1. Comparison of Lagrangian and Arbitrary Lagrangian-Eulerian mappings.
In this figure the demonstration of Lagrangian mapping (on the left) and ALE mapping (on the right) is shown. Although the Lagrangian mapping allows the structure to be deflected, the other (artificial) boundaries are also deformed , which is unusable in practical computations. ALE mapping is then the "compromise" between having fixed artificial boundaries and deflected the structure boundary.

2. Problem description

In this section the addresed aeroelastic model is presented. The fluid flow is described with the aid of the Reynolds Averaged Navier-Stokes(RANS) incompressible equations. The Reynolds stresses are modelled with the aid of the one equation Spallart-Almaras model. The aerodynamical forces are then evaluated and used in the structural model, which is presented here as the system of two ordinary differential equations. In order to describe the mathematical model for the case of moving meshes, the concept of Arbitrary Lagrangian-Eulerian formulation is briefly explained. The discretization of incompressible Navier-Stokes equations (INSE) can be considered as a special case of the RANS equations with turbulent viscosity ν_T set to $\nu_T \equiv 0$.

2.1. Arbitrary Lagrangian-Eulerian formulation

The numerical approximation of the time derivative by a time difference leads to complications in the case of time dependent domains and moving meshes. These complications are mainly caused by the fact that the grid points change their location during every time step. With the use of Arbitrary Lagrangian-Eulerian (ALE) method the original mathematical model can be reformulated in a suitable way and the finite element space discretization together with a suitable time discretization can be introduced. The ALE method is based on the definition of an ALE mapping of the original configuration computational domain $\mathcal{G}_0$ onto the computational domain $\mathcal{G}_t$ and the definition of the ALE domain velocity as the time derivative of the ALE mapping $\mathcal{A}_t$, i.e.

$$\mathcal{A}_t : \mathcal{G}_0 \mapsto \mathcal{G}_t, \qquad \tilde{\mathbf{w}}_g = \frac{\partial \mathcal{A}_t}{\partial t}, \qquad \mathbf{w}_g = \tilde{\mathbf{w}}_g \circ \mathcal{A}_t^{-1}.$$

With the aid of the time differentiation with respect to the original configuration $\mathcal{G}_0$, leading to the so-called ALE derivative denoted by $\frac{D^{\mathcal{A}_t}}{Dt}$, the time derivative of any function can be rewritten as $\frac{\partial}{\partial t} = \frac{D^{\mathcal{A}_t}}{Dt} - (\mathbf{w}_g \cdot \nabla)$. For more details about ALE method, see, e.g., (Nomura and Hughes, 1992).

2.2. Reynolds Averaged Navier-Stokes equations and turbulence modelling

Let us assume that at each time instant t the boundary $\mathcal{G}_t$ is split into three distjoint parts $\partial\mathcal{G}_t = \Gamma_D \cup \Gamma_O \cup \Gamma_{W_t}$. The turbulent fluid flow is modelled with the numerical solution of Reynolds Averaged Navier-Stokes equations

$$\frac{\partial U_i}{\partial t} - \nu \sum_j \frac{\partial}{\partial x_j} \left(\frac{\partial U_i}{\partial x_j} + \frac{\partial U_j}{\partial x_i} \right) + (\mathbf{U} \cdot \nabla) U_i + \frac{\partial P}{\partial x_i} = - \sum_j \frac{\partial}{\partial x_j} \overline{u_i' u_j'} + \mathbf{f}, \qquad \nabla \cdot \mathbf{U} = 0, \tag{1}$$

where the right hand side terms are so called Reynolds stresses $\sigma_{ij} = -\overline{u_i' u_j'}$.

The system (1) is equipped with the following boundary conditions

$$\begin{aligned} &\text{a)} \quad \mathbf{U} = \mathbf{U}_D, \quad \text{on } \Gamma_D, \\ &\text{b)} \quad \mathbf{U} = \mathbf{w}_g, \quad \text{on } \Gamma_{W_t}, \\ &\text{c)} \quad -\nu \sum_j \left(\frac{\partial U_i}{\partial x_j} + \frac{\partial U_j}{\partial x_i} \right) \mathbf{n}_j + (P - P_{ref})\mathbf{n}_i = \sum_j \sigma_{ij} \mathbf{n}_j, \quad \text{on } \Gamma_O, \end{aligned} \tag{2}$$

and with the initial condition $\mathbf{U}(x,0) = \mathbf{U}_0(x)$ for $x \in \mathcal{G}_0$. If we set $\sigma_{ij} \equiv 0$, then the boundary condition (2,c) is reduced to the well-known "do-nothing" boundary condition. The Reynolds stress tensor $\sigma = (\sigma_{ij})$ requires further modelling. One possibility is to use the Bousinesq assumption consisting of taking σ in the form

$$\sigma_{ij} = -\frac{2}{3} k \delta_{ij} + \nu_T \left(\frac{\partial U_i}{\partial x_j} + \frac{\partial U_j}{\partial x_i} \right)$$

In the present paper the turbulent kinematic viscosity is modelled with the aid of one-equation Spallart-Almaras model and the volumetric part $-\frac{2}{3}k\delta_{ij}$ is included in the pressure term. In this approach, the system of equations (1) is coupled with the following nonlinear partial differential equation

$$\frac{D^{\mathcal{A}_t} \tilde{\nu}}{Dt} + ((\mathbf{U} - \mathbf{w}_g) \cdot \nabla) \tilde{\nu} = \frac{1}{\beta} \left[\sum_{i=1}^{2} \frac{\partial}{\partial x_i} \left((\nu + \tilde{\nu}) \frac{\partial \tilde{\nu}}{\partial x_i} \right) + c_{b_2} (\nabla \tilde{\nu})^2 \right] + G - Y, \tag{3}$$

equipped with the boundary conditions $\tilde{\nu} = 0$ on Γ_{W_t} and $\frac{\partial \tilde{\nu}}{\partial \mathbf{n}} = 0$ on $\Gamma_O \cup \Gamma_D$. The functions G and Y are functions of the tensor of rotation of mean velocity Ω and of the wall distance y, i.e.

$$G = c_{b_1} \tilde{S} \cdot \tilde{\nu}, \qquad Y = c_{w_1} \frac{\tilde{\nu}^2}{y^2} \left(\frac{1+c_{w_3}^6}{1+c_{w_3}^6/g^6} \right)^{\frac{1}{6}}, \qquad \tilde{S} = \left(S + \frac{\tilde{\nu}}{\kappa^2 y^2} f_{v_2} \right), \qquad f_{v_2} = 1 - \frac{\chi}{1+\chi f_{v_1}},$$
$$g = r + c_{w_2}(r^6 - r), \qquad r = \frac{\tilde{\nu}}{\tilde{S}\kappa^2 y^2}, \qquad S = \sqrt{2\Omega(\mathbf{U}) : \Omega(\mathbf{U})}, \qquad \Omega(\mathbf{U}) = \tfrac{1}{2}(\nabla \mathbf{U} - \nabla \mathbf{U}^T).$$

The following choice of constants is used

$$c_{b_1} = 0.1355, \qquad c_{b_2} = 0.622, \qquad \beta = \frac{2}{3}, \qquad c_v = 7.1,$$

$$c_{w_3} = 0.3, \quad c_{w_3} = 2.0, \quad \kappa = 0.41, \quad c_{w_1} = c_{b_1}/\kappa^2 + (1 + c_{b_2})/\beta.$$

The Reynolds stresses then are computed as

$$\sigma_{ij} = -\nu_T \left(\frac{\partial U_i}{\partial x_j} + \frac{\partial U_j}{\partial x_i} \right), \quad \nu_T = \tilde{\nu} \frac{\chi^3}{\chi^3 + c_v^3}, \quad \chi = \frac{\tilde{\nu}}{\nu},$$

where the volumetric part of σ has been included in the pressure term, i.e. $P^* = P + \frac{2}{3}k$. In what follows we shall not distinguish between P and P^*, we shall simply use the symbol P.

The space discretization of the problem is carried out by the finite element method, which starts from the so called weak formulation. To this end we introduce the velocity spaces W, X, the pressure space Q and the turbulence model space Λ:

$$W = (H^1(\mathcal{G}_t))^2, \quad X = \{\mathbf{v} \in W; \mathbf{v}|_{\Gamma_D \cup \Gamma_{Wt}} = 0\}, \quad Q = L^2(\mathcal{G}_t), \quad \Lambda = \{\phi \in W; \phi|_{\Gamma_{Wt}} = 0\}$$

where $L^2(\mathcal{G}_t)$ is the Lebesgue space of square integrable functions over the domain $\mathcal{G}_t$ and $H^1(\mathcal{G}_t)$ is the Sobolev space of functions square integrable together with their first order derivatives.

Now, multiplying the system of equation (1) by test functions $\mathbf{v} \in X$ and $q \in Q$, integrating over the domain $\mathcal{G}_t$ and using Green's theorem, we obtain the weak formulation: find $\mathbf{U} : \langle 0, T \rangle \mapsto W$ such that for all t the Dirichlet boundary conditions (2 a-b) are satisfied and $P : \langle 0, T \rangle \mapsto Q$ such that for all $t \in \langle 0, T \rangle$ the following equality holds

$$\mathbf{a}(\mathbf{U} - \mathbf{w}_g; \mathbf{U}, P; \mathbf{v}, q) = \mathbf{L}(\mathbf{v}, q), \qquad \forall \mathbf{v} \in X, q \in Q \tag{4}$$

where

$$\begin{aligned} \mathbf{a}(\mathbf{b}; \mathbf{U}, P; \mathbf{v}, q) &= \left(\frac{D^{\mathcal{A}_t} \mathbf{U}}{Dt}, \mathbf{v} \right)_{\mathcal{G}_t} + \nu \Big(\nabla \mathbf{U}, \nabla \mathbf{v} \Big)_{\mathcal{G}_t} + \sum_{i,j} \left(\sigma_{ij}(\mathbf{U}), \frac{\partial \mathbf{v}_i}{\partial x_j} \right)_{\mathcal{G}_t} \\ &\quad + \Big((\mathbf{b} \cdot \nabla) \mathbf{U}, \mathbf{v} \Big)_{\mathcal{G}_t} - \Big(P, \nabla \cdot \mathbf{v} \Big)_{\mathcal{G}_t} + \Big(\nabla \cdot \mathbf{U}, q \Big)_{\mathcal{G}_t}, \\ \mathbf{L}(\mathbf{v}, q) &= (\mathbf{f}, \mathbf{v})_{\mathcal{G}_t}. \end{aligned}$$

Now, by multiplying the equation (3) by a test function $\phi \in \Lambda$, integrating over the domain $\mathcal{G}_t$ and using the Green's theorem, we obtain the weak formulation of the Spallart-Almaras turbulence one-equation model: Find $\tilde{\nu} : [0,T] \mapsto \Lambda$ such that for all $\phi \in \Lambda$ and for any time $t \in [0,T]$ the following equation holds

$$\left(\frac{D^{\mathcal{A}_t}\tilde{\nu}}{Dt}, \phi\right)_{\mathcal{G}_t} + \left((\mathbf{U}-\mathbf{w}_g)\cdot\nabla\tilde{\nu}, \phi\right)_{\mathcal{G}_t} + \left((\nu+\tilde{\nu})\nabla\tilde{\nu}, \nabla\psi\right)_{\mathcal{G}_t} + (Y,\psi)_{\mathcal{G}_t} = (G,\psi)_{\mathcal{G}_t} + \left(\frac{c_{b_2}}{\beta}(\nabla\tilde{\nu})^2, \psi\right). \tag{5}$$

2.3. Structural model and fluid-structure coupling

The nonlinear equations of motion for a flexibly supported body, see (Sváček, Feistauer, and Horáček, 2004), read

$$\begin{aligned} m\,\ddot{h} + S_\alpha\,\ddot{\alpha}\,\cos\alpha - S_\alpha\,\dot{\alpha}^2\,\sin\alpha + k_{hh}\,h &= -L(t), \\ S_\alpha\,\ddot{h}\,\cos\alpha + I_\alpha\ddot{\alpha} + k_{\alpha\alpha}\,\alpha &= M(t), \end{aligned} \tag{6}$$

where the possibility of large values of α and h have been considered. For small values of the angle α, when $\alpha \approx 0$, $\sin\alpha \approx 0$ and $\cos\alpha \approx 1$, the system (6) can be rewritten in a simplified form (see, e.g., (Dowell, 1995), (Naudasher and Rockwell, 1994)). The aerodynamical forces acting on the airfoil can be evaluated

$$L = -\int_{\Gamma_{W_t}} \sum_{j=1}^{2} \tau_{2j} n_j dS, \qquad M = -\int_{\Gamma_{W_t}} \sum_{i,j=1}^{2} \tau_{ij} n_j r_i^{\mathrm{ort}} dS, \tag{7}$$

$$\tag{8}$$

where $r_1^{\mathrm{ort}} = -(x_2 - x_{EO2})$, $r_2^{\mathrm{ort}} = x_1 - x_{EO1}$ and τ is the stress tensor, i.e.

$$\tau_{ij} = \rho\left[p\delta_{ij} + \nu\left(\frac{\partial U_i}{\partial x_j} + \frac{\partial U_j}{\partial x_i}\right)\right].$$

One should notice that the fluid flow model (1) and the structural model (6) can not be solved independently: clearly the aerodynamical forces $L(t)$ and $M(t)$, determined by the solution of the fluid flow model, appear in right hand side of (6) and, on the other hand, the deformation of the computational domain $\mathcal{G}_t$ depends on the angle of rotation $\alpha = \alpha(t)$ and the translation $h = h(t)$, which form the solution of the system (6).

3. Discretization of the problem

3.1. Space-time discretization

First, we start with time partition $0 = t_0 < t_1 < \cdots < T$, $t_k = k\Delta t$, with a time step $\Delta t > 0$ and approximate the function $\mathbf{U}(t_n)$, $P(t_n)$ and $\tilde{\nu}(t_n)$ defined in $\mathcal{G}_{t_n}$ at time t_n by $\mathbf{U}^n$, P^n and $\tilde{\nu}^n$. The ALE derivative can approximated by the finite differences

$$\left.\frac{D^{\mathcal{A}}\mathbf{u}}{Dt}\right|_{t^{n+1}} = \frac{3\mathbf{u}^{n+1} - 4\hat{\mathbf{u}}^n + \hat{\mathbf{u}}^{n-1}}{2\Delta t}, \qquad \left.\frac{D^{\mathcal{A}}\tilde{\nu}}{Dt}\right|_{t^{n+1}} = \frac{3\tilde{\nu}^{n+1} - 4\hat{\tilde{\nu}}^n + \hat{\tilde{\nu}}^{n-1}}{2\Delta t}, \tag{9}$$

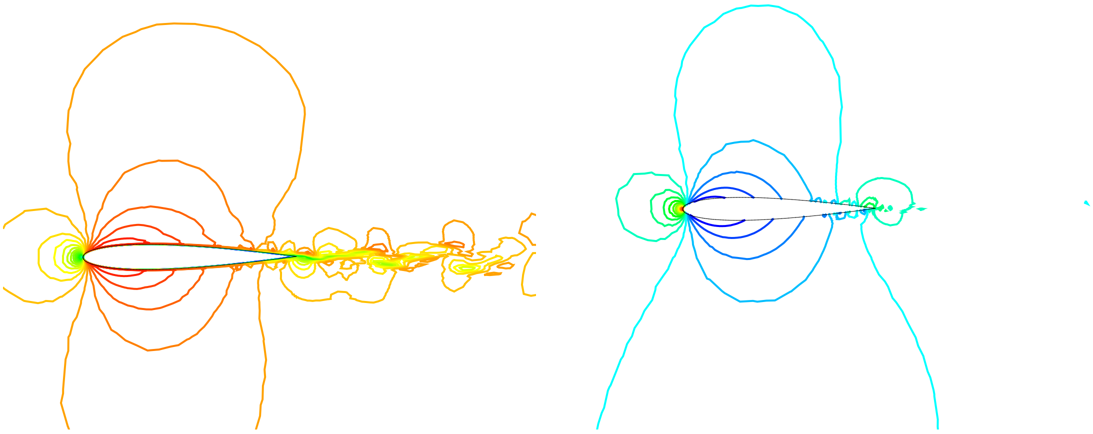

Figure 2. The fluid velocity and pressure isolines for inlet velocity $U = 25 m\, s^{-1}$

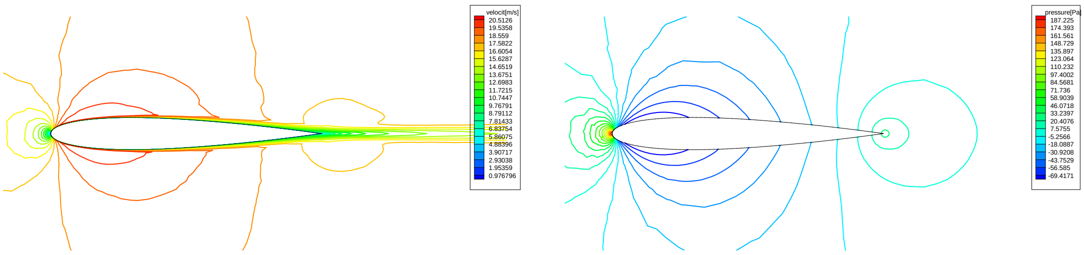

Figure 3. The time averaged fluid velocity and pressure isolines for inlet velocity $U = 25 m\, s^{-1}$, stationary solution.

where for a function $f : \mathcal{G}_i \mapsto R$ the function $\hat{f}^i : \mathcal{G}_{n+1} \mapsto R$ is defined as $\hat{f}^i = f \circ \mathcal{A}_{t_i} \circ \mathcal{A}^{-1}_{t_{n+1}}$ at a fixed time step t_{n+1}. Then the form $\mathbf{a}$ is modified in the following way:

$$
\begin{aligned}
\mathbf{a}(\mathbf{b};\mathbf{U},P;\mathbf{v},q) &= \left(\frac{3\mathbf{U}^{n+1}}{2\Delta t},\mathbf{v}\right)_{\mathcal{G}_{n+1}} + \nu\left(\nabla\mathbf{U},\nabla\mathbf{v}\right)_{\mathcal{G}_{n+1}} + \sum_{i,j}\left(\sigma_{ij}(\mathbf{U}),\frac{\partial \mathbf{v}_i}{\partial x_j}\right)_{\mathcal{G}_{n+1}} \\
&\quad + \left((\mathbf{b}\cdot\nabla)\mathbf{U},\mathbf{v}\right)_{\mathcal{G}_{n+1}} - \left(P,\nabla\cdot\mathbf{v}\right)_{\mathcal{G}_{n+1}} + \left(\nabla\cdot\mathbf{U},q\right)_{\mathcal{G}_{n+1}}, \\
\mathbf{L}(\mathbf{v},q) &= \left(\frac{4\hat{\mathbf{U}}^{n} - \hat{\mathbf{U}}^{n-1}}{2\Delta t},\mathbf{v}\right)_{\mathcal{G}_{n+1}},
\end{aligned}
$$

and the semi-implicit weak form of the Spallart-Almaras turbulence reads: Find $\tilde{\nu}^{n+1} \in \Lambda$ such that for all $\phi \in \Lambda$ holds the following equation

$$\mathbf{c}(\tilde{\nu}^{n+1},\phi) = \mathbf{l}(\phi), \tag{10}$$

where

$$\mathbf{c}(\tilde{\nu}^{n+1},\phi)=\Big(\frac{3\tilde{\nu}^{n+1}}{2\Delta t},\phi\Big)_{\mathcal{G}_{n+1}}+\Big((\mathbf{U}^{n+1}-\mathbf{w}_g)\cdot\nabla\tilde{\nu}^{n+1},\phi\Big)_{\mathcal{G}_{n+1}}+\Big(\frac{\nu+\tilde{\nu}^n}{\beta}\nabla\tilde{\nu}^{n+1},\nabla\phi\Big)_{\mathcal{G}_{n+1}}+\Big(s^{(n)}\tilde{\nu}^{n+1},\nabla\phi\Big)_{\mathcal{G}_{n+1}}$$

$$\mathbf{l}(\phi)=\left(\frac{4\hat{\tilde{\nu}}^n-\hat{\tilde{\nu}}^{n-1}}{2\Delta t},\phi\right)_{\mathcal{G}_{n+1}}+\left(G^{(n)},\phi\right)_{\mathcal{G}_{n+1}}+\left(\frac{c_{b_2}}{\beta}(\nabla\hat{\tilde{\nu}}^n)^2,\phi\right)_{\mathcal{G}_{n+1}},$$

and

$$s^{(n)}=c_{w_1}\frac{\tilde{\nu}^n}{y^2}\left(\frac{1+c_{w_3}^6}{1+c_{w_3}^6/g^6}\right)^{1/6},\qquad G^{(n)}=c_{b_1}\overline{S}\hat{\tilde{\nu}}^n.$$

In order to apply the Galerkin FEM, we approximate the spaces W, X, Q from the weak formulation by finite dimensional subspaces $W_\Delta\subset W$, $Q_\Delta\subset Q$, $\Lambda_\Delta\subset\Lambda$ for $\Delta\in(0,\Delta_0)$ and we set

$$X_\Delta=\{\mathbf{v}_\Delta\in W_\Delta;\mathbf{v}_\Delta|_{\Gamma_D\cap\Gamma_{Wt}}=0\}.$$

Hence, we define the *discrete problem* to find an approximate solution $\mathbf{U}_\Delta\in W_\Delta$ and $P_\Delta\in Q_\Delta$ such that $\mathbf{U}_\Delta$ satisfies approximately boundary conditions and the identity

$$a(\mathbf{U}-\mathbf{w}_g;\mathbf{U},P;\mathbf{v},q)=\mathbf{L}(\mathbf{v},q),\qquad\forall\mathbf{v},q \tag{11}$$

The couple (X_Δ,Q_Δ) of the finite element spaces should satisfy the *Babuška-Brezzi (BB) inf-sup condition* (see, e.g. (Girault and Raviart, 1986)). In our computations, the well-known Taylor-Hood P_2/P_1 conforming elements on triangular meshes are used for the velocity/pressure approximation.

The standard Galerkin discretization (11) may produce approximate solutions suffering from spurious oscillations for high Reynolds numbers. In order to avoid this drawback, the stabilization via *Galerkin Least-Squares technique* is applied (see, e.g. (Lube, 1994), (Gelhard, Lube, and Olshanskii, 2003)). The stabilization terms are defined as

$$\begin{aligned}\mathcal{L}_\Delta(\mathbf{b};\mathbf{U},p;\mathbf{v},q)&=\sum_{K\in\mathcal{T}_\Delta}\sum_{i=1}^{2}\delta_K\left(\frac{3}{2\Delta t}U_i-\nu\triangle U_i+(\mathbf{b}\cdot\nabla)U_i+\frac{\partial P}{\partial x_i}-\sum_{j=1}^{2}\frac{\partial\sigma_{ij}(\mathbf{U})}{\partial x_j},(\mathbf{b}\cdot\nabla)v_i+\frac{\partial q}{\partial x_i}\right)_K,\\ \mathcal{F}_\Delta(\mathbf{v})&=\sum_{K\in\mathcal{T}_\Delta}\sum_{i=1}^{2}\delta_K\left(\frac{4\hat{U}_i^{\,n}-\hat{U}_i^{\,n-1}}{2\Delta t}+\mathbf{f}_i,(\mathbf{b}\cdot\nabla)v_i+\frac{\partial q}{\partial x_i}\right)_K,\end{aligned}\tag{12}$$

and the additional grad-div stabilization terms

$$\mathcal{P}_\Delta(\mathbf{U},\mathbf{v})=\sum_{K\in\mathcal{T}_\Delta}\tau_K(\nabla\cdot\mathbf{U},\nabla\cdot\mathbf{v})_K, \tag{13}$$

are introduced with suitably chosen parameters $\delta_K\geq 0$ and $\tau_K\geq 0$.

The *stabilized discrete problem* reads: Find $\mathbf{U}_\Delta\in W_\Delta$ and $P_\Delta\times Q_\Delta$ such that $\mathbf{U}_\Delta$ satisfies approximately conditions (2), a), b) and

$$\mathbf{a}(\mathbf{U}-\mathbf{w}_g;\mathbf{U},P;\mathbf{v},q)+\mathcal{L}_\Delta(\mathbf{U}-\mathbf{w}_g;\mathbf{U},P;\mathbf{v},q)+\mathcal{P}_\Delta(\mathbf{U},\mathbf{v})=\mathbf{L}(\mathbf{v},q)+\mathcal{F}_\Delta(V_\Delta)$$
$$\text{for all }\mathbf{v}_\Delta\in X_\Delta,q_\Delta)\in Q_\Delta. \tag{14}$$

Furthermore, the approximate solution of the RANS system (1) is coupled with the Spallart-Almaras turbulence model given by the solution of (10). The nonlinear algebraic discrete system (14) and (10) is solved on each time level t_{n+1} with the aid of the linearized Oseen iterative process. More detailed description of Oseen iterative process can be found in (Sváček, Feistauer, and Horáček, 2004) for (laminar) Navier-Stokes equations.

4. Numerical results. Conclusions

In this paper we present the comparison of the presented method with NASTRAN computation and with the numerical simulation with the aid of Spallart-Almaras turbulence model. The parameters of the structural model was set as

$$m = 0.086622 \text{ kg}, \quad S_\alpha = -0.000779673 \text{ kg m}, \quad I_\alpha = 0.000487291 \text{ kg m}^2,$$
$$k_{hh} = 105.109 \text{ N m}^{-1}, \quad k_{\alpha\alpha} = 3.695582 \text{ N m rad}^{-1}, \quad l = 0.05 \text{ m}, \quad c = 0.3 \text{ m}.$$

The elastic axis is located at 40% of the airfoil, $\rho = 1.225$ kg m^{-3}, $\nu = 1.5 \cdot 10^{-5}$ m s^{-2}. The numerical computations were performed for airfoils NACA 0012 (turbulent case) and NACA $63_2 -$ 415 (laminar case).

First, the numerical approximation of the coupled model with RANS equations was obtained for velocities in the range $5 - 40$ m s^{-1}. The aeroelastic responses of the airfoil are shown in Figures 4, 5 and 6 for different values of the far field velocity U_∞ in the stable region. In Figure 7 the aeroelastic response for far field velocity $U_\infty = 38$m s^{-1} is shown, where the coupled model is unstable (This is in agreement with NASTRAN computations by STRIP model, where the determined critical velocity was shown for $U_\infty = 37.7$m s^{-1}. In Figure 8 the comparison of the frequencies and damping coefficient determined from the aeroelastic response of the coupled model and frequencies and damping coefficient from NASTRAN computations (see (Čečrdle and Maleček, 2002)) is shown.

The similar computations were performed for (laminar) Navier-Stokes equations and the flow over an airfoil NACA $63_2 - 415$. Figure 9 shows the behaviour of the coupled model in this case. The post-flutter behaviour in this case is shown in Figure 10. In order to validate the results for large large structural displacements the numerical simulation of vibrating airfoil was performed and compared to the experimental results. Figure 11 shows the streamlines patterns, which is in good agreement to the experimental results, see Naudasher and Rockwell, Figure 7.11.

The result shows that both laminar and turbulent approximation of fluid flow leads to comparable results, the determined critical velocity by the presented method is in agreement with the NASTRAN computation (Čečrdle and Maleček, 2002). The main difference is demonstrated in Figures 2 and 3, where for the turbulence model leads to the stationary solution in the case of fixed airfoil, which is not the case of 'laminar' simulations.

References

Čečrdle J. and Maleček J. Verification FEM model of an aircraft construction with two and three degrees of freedom. *Tech. Rep. Research Report R-3418/02*, Aeronautical Research and Test Institute, Prague, Letňany, 2002.

Dobeš, J., Ricchiuto, M., Deconinck, H., 2005. Implicit space-time residual distribution method for unsteady laminar viscous flows. *Computers and Fluids* 34 (4-5), 593–616, 2005.

Dolejší, V. Anisotropic mesh adaptation technique for viscous flow simulation. *East-West Journal of Numerical Mathematics* 9 (1), 1–24, 2001

Dowell, E. H., A Modern Course in Aeroelasticity. Kluwer Academic Publishers, Dodrecht, 1995

Gelhard, T., Lube, G., Olshanskii, M. A., 2004. Stabilized finite element schemes with LBB-stable elements for incompressible flows. *Journal of Computational and Applied Mathematics* (accepted).

Girault, V., Raviart, P.-A., Finite Element Methods for the Navier-Stokes Equations. Springer-Verlag, Berlin, 1986.

LeTallec, P., Mouro, J., 1998. Fluid structure interaction with large structural displacements. In: 4th ECCOMASS Computational Fluid Dynamics Conference. pp. 1032–1039, 1998

Lube, G., 1994. Stabilized Galerkin finite element methods for convection dominated and incompressible flow problems. *Numerical Analysis and Mathematical Modelling* 29, 85–104, 1994

Naudasher, E., Rockwell, D. Flow-Induced Vibrations A.A. Balkema, Rotterdam, 1994.

Nomura, T., Hughes, T. J. R., An arbitrary Lagrangian-Eulerian finite element method for interaction of fluid and a rigid body. *Computer Methods in Applied Mechanics and Engineering* 95, 115–138, 1992

Sváček, P., Feistauer, M. Application of a stabilized FEM to problems of aeroelasticity. In: Feistauer, M., Dolejší, V., K., N. (Eds.),*Numerical Mathematics and Advanced Applications*, ENUMATH2003. Springer, Heidelberg, pp. 796–805, 2004

Sváček, P. , Feistauer, M., Horáček, J., Numerical simulation of flow induced airfoil vibrations with large amplitudes. *Journal of Fluids and Structures*(submitted).

Wilcox, D. C., 1993. Turbulence Modeling for CFD. DCW Industries.

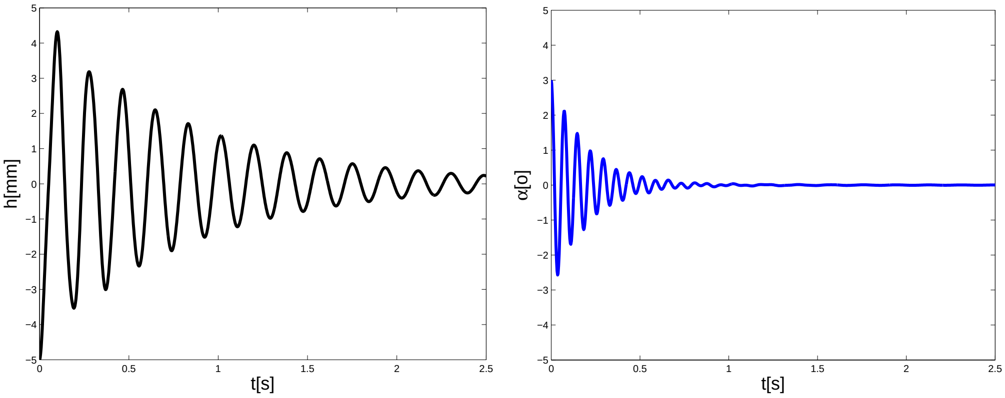

$U_\infty = 5 \text{ m s}^{-1}$

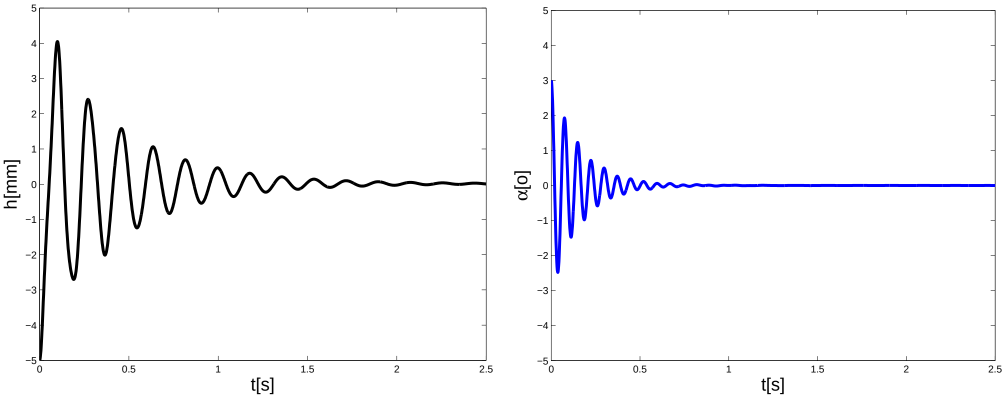

$U_\infty = 10 \text{ m s}^{-1}$

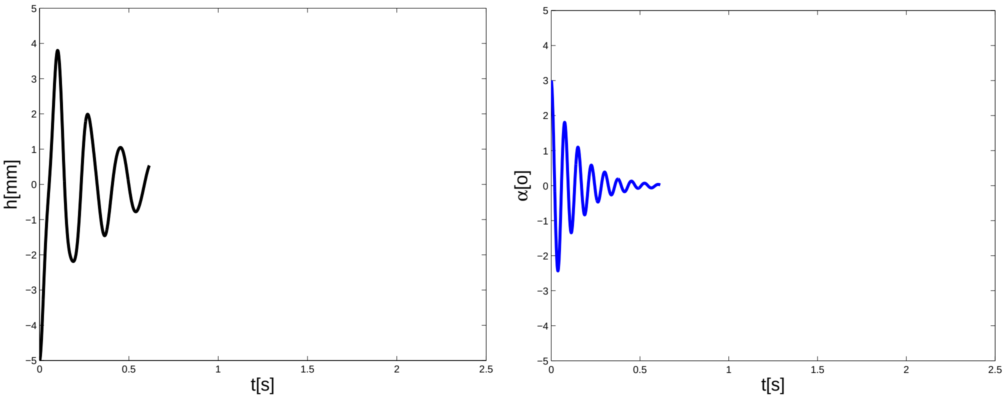

$U_\infty = 12,5 \text{ m s}^{-1}$

Figure 4. RANS simulations with Spallart-Almaras turbulence model for $U_\infty = 5, 10,$ and 12.5 m s^{-1}
The graph of the airfoil displacements in h (on the left) and α (on the right). In this case the coupled model is in stable region and two main frequencies can be identified in the aeroelastic response of the airfoil. Futhermore, with increasing far field velocity the aerodynamical damping is increasing.

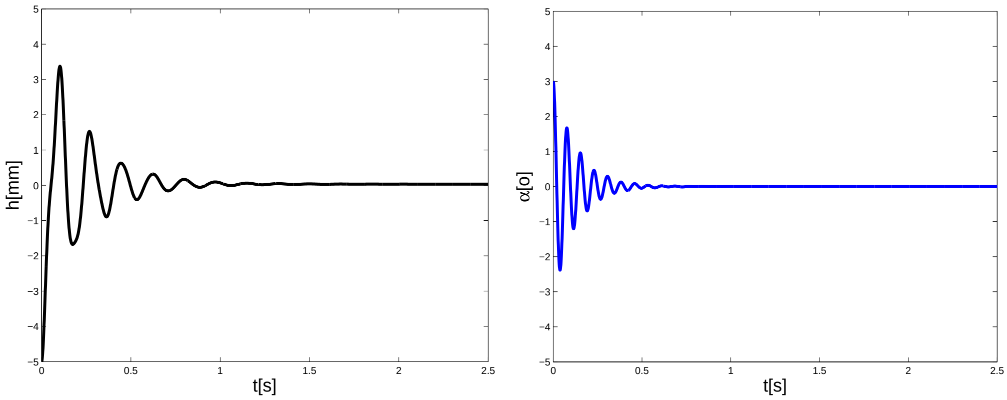

$U_\infty = 15 \text{ m s}^{-1}$

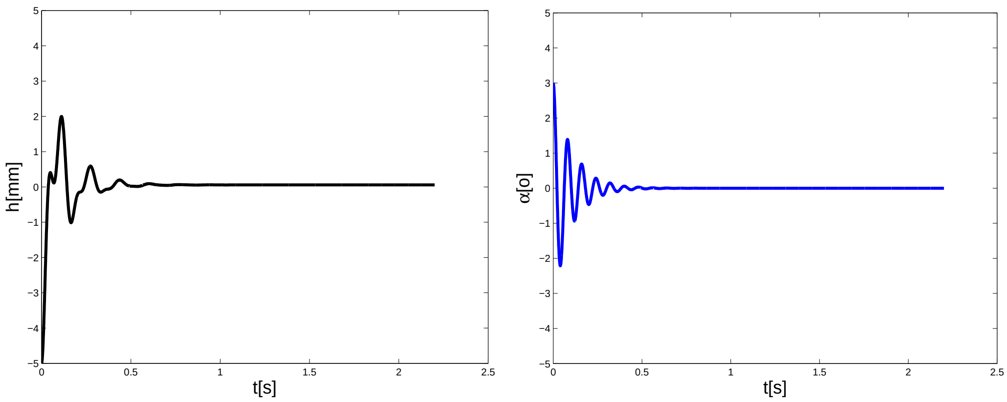

$U_\infty = 20 \text{ m s}^{-1}$

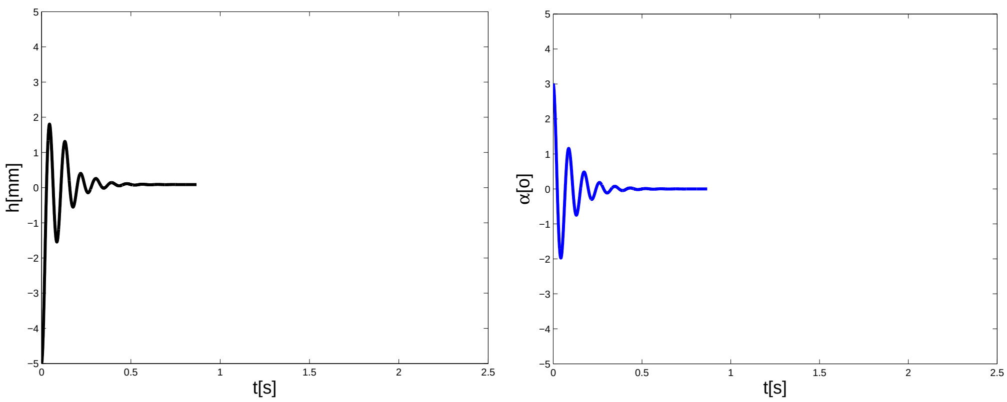

$U_\infty = 25 \text{ m s}^{-1}$

Figure 5. RANS simulations with Spallart-Almaras turbulence model for field velocity $U_\infty = 15, 20, 25 \text{ m s}^{-1}$
The graph of the airfoil displacements in h (on the left) and α (on the right). The aeroelastic behaviour is still in stable region, two main frequencies can be identified, for far field velocity $U_\infty = 25 \text{ m s}^{-1}$ the aerodynamical damping is maximal.

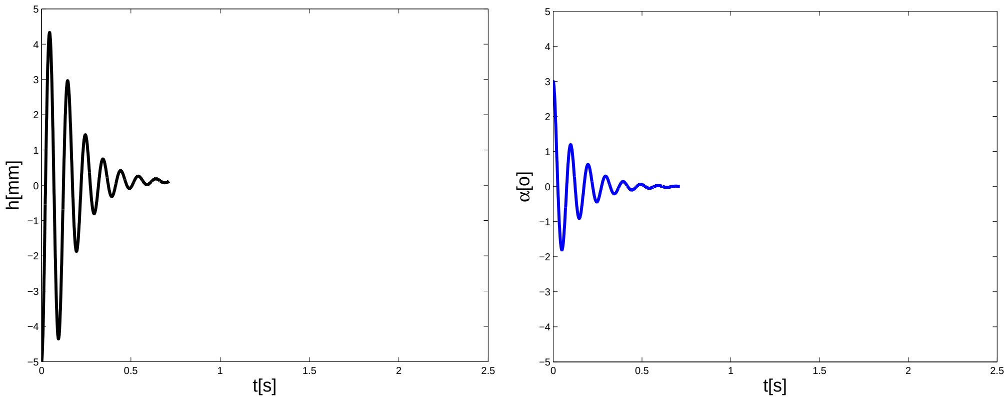

$$U_\infty = 30 \text{ m s}^{-1}$$

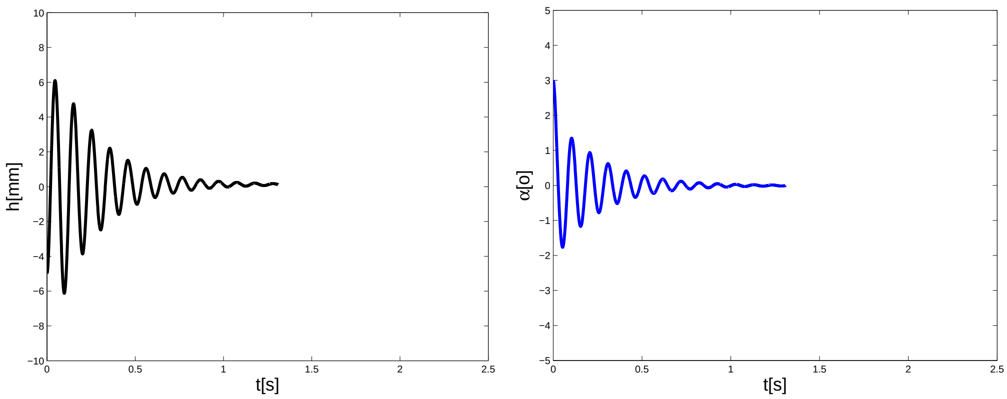

$$U_\infty = 32.5 \text{ m s}^{-1}$$

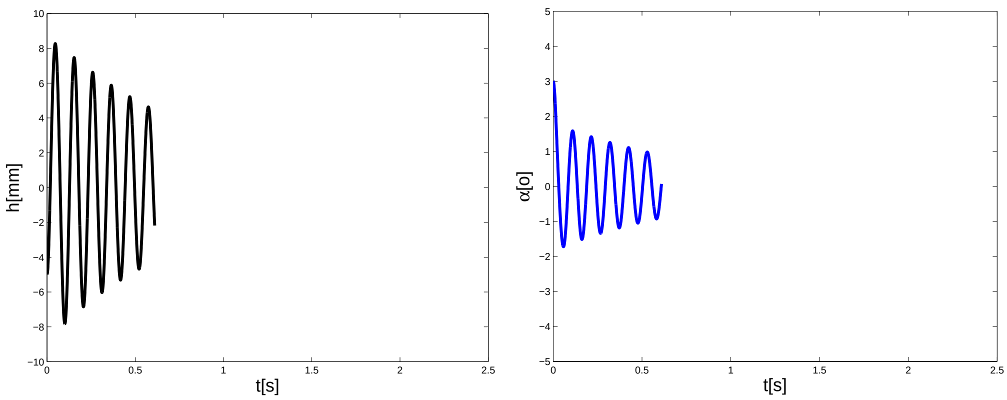

$$U_\infty = 35 \text{ m s}^{-1}$$

Figure 6. RANS simulations with Spallart-Almaras turbulence model for $U_\infty = 30, 32, 35$ m s^{-1}
The graph of the airfoil displacements in h (on the left) and α (on the right). In this region of velocities only one frequency can be identified in the aeroelastic response of the airfoil and with increasing far field velocity the aerodynamical damping starts to be decreasing.

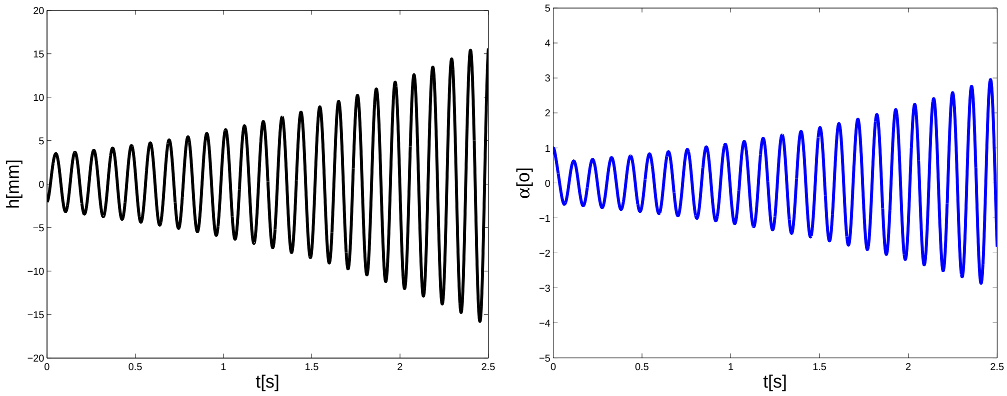

Figure 7. RANS simulations with Spallart-Almaras turbulence model for post-critical velocity $U_\infty = 38$ m s^{-1} For this value of far field velocity the aeroelastic problem is unstable, the vibrations slowly increases in time.

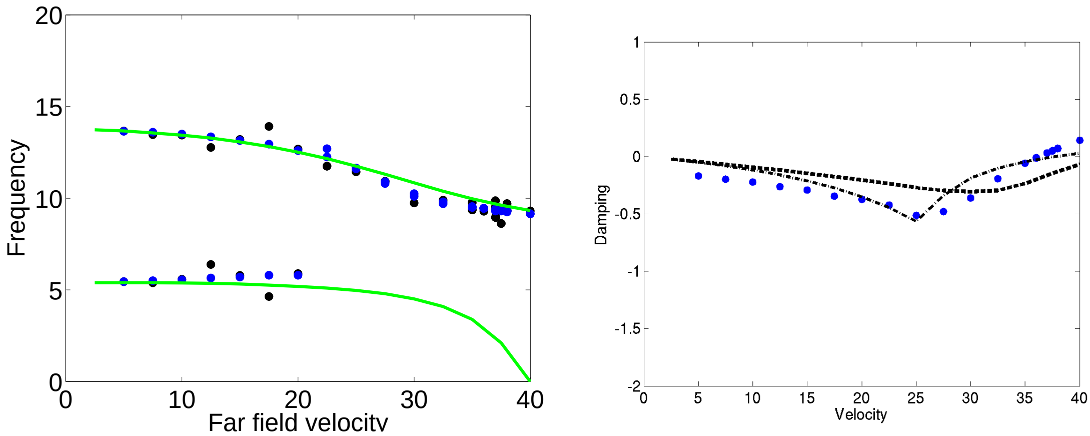

Figure 8. Comparison of frequency and damping for the aeroelastic response for the presented FE simulations of RANS equations and NASTRAN computations.

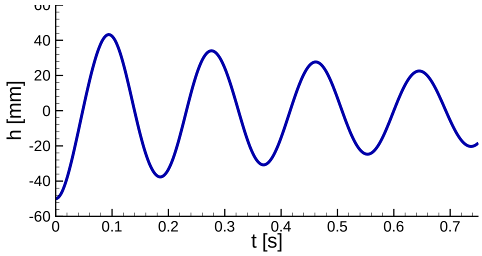

$U_\infty = 4$ m s^{-1}

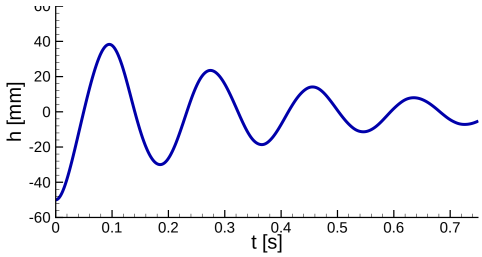

$U_\infty = 10$ m s^{-1}

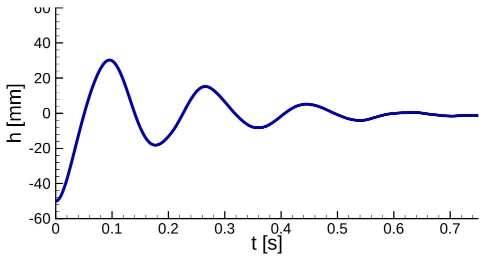

$U_\infty = 16$ m s^{-1}

Figure 9. Navier-Stokes equations (laminar) simulations for the aeroelastic simulations and subcritical velocity $U_\infty = 5, 10,$ and 16 m s^{-1}
The graph of the airfoil displacements in h (on the left) and α (on the right). In this case the coupled model is in stable region and two main frequencies can be identified in the aeroelastic response of the airfoil. Futhermore, with increasing far field velocity the aerodynamical damping is increasing. For the far field velocity $U_\infty = 16$ m s^{-1} the vibrations are not fully damped as it was the case for the RANS simulations, but the aeroelastic model still remains clearly stable.

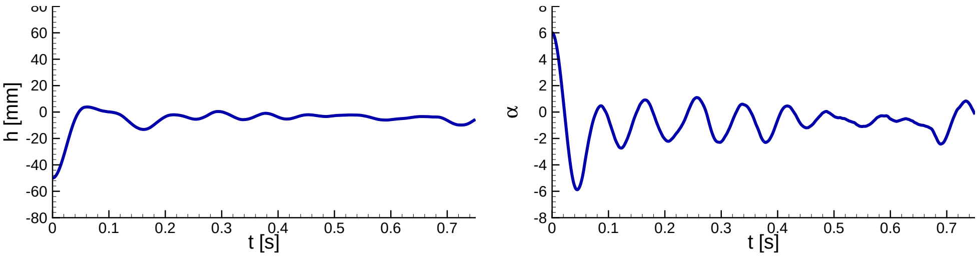

$U_\infty = 30 \text{ m s}^{-1}$

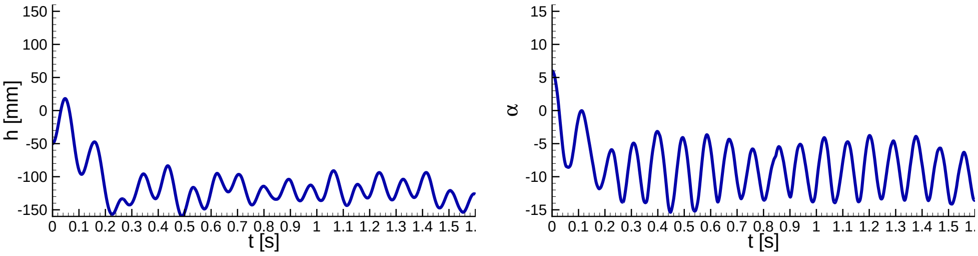

$U_\infty = 40 \text{ m s}^{-1}$

Figure 10. Navier-Stokes equations (laminar) simulations for the aeroelastic simulations and for sub-critical velocity $U_\infty = 30 \text{ m s}^{-1}$ and for post-critical velocity $U_\infty = 40 \text{ m s}^{-1}$

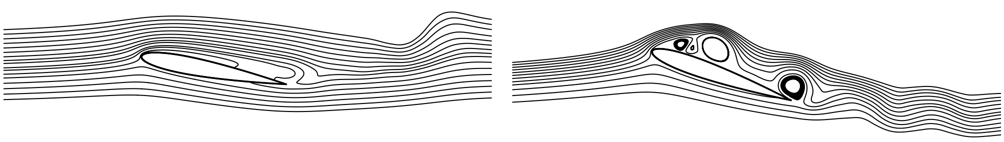

$\alpha = 10.859$ $\alpha = 19.4553$

Figure 11. Incompressible (laminar) Navier-Stokes equations simulations.
Instantaneous streamline patterns for vibrating airfoil $Re = 5000$, $\alpha = 10° + 10° \sin(2\pi f_s t)$ at $f_s c/U_\infty = 1/2\pi$ showing the 'dynamic stall vortex' (after (Naudasher and Rockwell, 1994))